Supplemental Materials

Molecular Biology of the Cell

Finnigan et al.

SUPPORTING INFORMATION

for

Coordinate action of distinct sequence elements localizes checkpoint kinase Hsl1 to the septin collar at the bud neck in *Saccharomyces cerevisiae*

Gregory C. Finnigan,[1] Sarah M. Sterling,[1] Angela Duvalyan,[1] Elizabeth N. Liao,[1] Aspram Sargsyan,[1] Galo Garcia III,[1†] Eva Nogales,[1,2,3] and Jeremy Thorner[1*]

[1]Division of Biochemistry, Biophysics and Structural Biology, Department of Molecular and Cell Biology, University of California, Berkeley, CA 94720-3202 USA;

[2]Life Sciences Division, Lawrence Berkeley National Laboratory, Berkeley, CA 94720 USA;

[3]Howard Hughes Medical Institute

Table S1. Yeast strains used to obtain the data in Figures S1 to S7.

Strain	Genotype	Reference
BY4741	*MAT**a** leu2Δ ura3Δ met15Δ his3Δ*	(Brachmann et al., 1998)
GFY-42	BY4741 *cdc10Δ::CDC10::mCherry::SpHIS5*	(Finnigan et al., 2015b)
GFY-1507[a]	BY4742 *msn5Δ::Kan^R*	Life Technologies, Inc.
GFY-1506[a]	BY4742 *los1Δ::Kan^R*	Life Technologies, Inc.
GFY-1537[b]	*MAT**a** ade2-101 his3-11,15 trp1-901 ura3-52 cse1-1 + pGF-IVL774*	This study
GFY-1539[b]	*MATα ade2-1 LYS2 leu2-3,112 trp1-1 can1-100 ura3-1 his3-11,15 xpo1::LEU2 + pKW457 [pRS313-xpo1-1ts] + pGF-IVL774*	This study
GFY-1541[c]	BY4741 *hsl1Δ::Kan^R*	This study
GFY-39	BY4741 *shs1Δ::Hyg^R*	This study
GFY-1451	BY4741 *shs1Δ::Hyg^R hsl1Δ::Kan^R*	This study
GFY-1120[d]	BY4741 *cdc11Δ::cdc11(G29D)::mCherry::Nat^R* + *pJT1520*	This study
GFY-1450	BY4741 *cdc11Δ::cdc11(G29D)::mCherry::Nat^R hsl1Δ::Kan^R + pJT1520*	This study
GFY-1430[e]	BY4741 *cdc12Δ::cdc12(K392N; Δ393-407)::mCherry::SpHIS5* + pJT1622	This study
GFY-1449	BY4741 *cdc12Δ::cdc12(K392N; Δ393-407)::mCherry::SpHIS5 hsl1Δ::Kan^R* + pJT1622	This study
GFY-1156	BY4741 *cdc10Δ::CDC10::mCherry::SpHIS5 hsl1Δ::Kan^R*	This study
GFY-768[f]	BY4741 *cdc11Δ::CDC11::mCherry::SpHIS5*	(Finnigan et al., 2015b)
GFY-1157	BY4741 *cdc11Δ::CDC11::mCherry::SpHIS5 hsl1Δ::Kan^R*	This study
GFY-104[g]	BY4741 *cdc12Δ::cdc12(K392N; Δ393-407)::mCherry::Kan^R* + pJT1622	(Finnigan et al., 2015a)
GFY-1561[h,i]	BY4741 *cdc10Δ::CDC10::mCherry::SpHIS5 hsl1Δ::HSL1(1-1518)::HA$_3$::Nat^R*	This study
GFY-1562[h]	BY4741 *cdc10Δ::CDC10::mCherry::SpHIS5 hsl1Δ::hsl1(1-1043; 1201-1518)::HA$_3$::Nat^R*	This study

GFY-1563[h]	BY4741 *cdc10Δ::CDC10::mCherry::SpHIS5 hsl1Δ:: hsl1(1-950; 1044-1518)::HA$_3$::Nat^R*	This study
GFY-1564[h]	BY4741 *cdc10Δ::CDC10::mCherry::SpHIS5 hsl1Δ:: hsl1(1-950; 1201-1518)::HA$_3$::Nat^R*	This study
GFY-1565[h]	BY4741 *cdc10Δ::CDC10::mCherry::SpHIS5 hsl1Δ:: hsl1(1-950; 1358-1518)::HA$_3$::Nat^R*	This study
GFY-1566[h]	BY4741 *cdc10Δ::CDC10::mCherry::SpHIS5 hsl1Δ:: hsl1(1-1043; 1358-1518)::HA$_3$::Nat^R*	This study

[a]These strains are clonal isolates obtained from the genome deletion collection (*MAT**α***) and confirmed using multiple diagnostic PCRs.

[b]Strains KWY125 and KWY121 (Strahl et al., 2005) were transformed with plasmid pGF-IVL774 and selected on SD-URA plates. Spontaneous white colonies were selected as clonal isolates (although the nature of the adenine pathway mutation(s) were not identified). Strain KWY125 was confirmed as cold sensitive (11-12°C) while strain KWY121 was confirmed as heat sensitive (37°C).

[c]This strain is a clonal isolate from the haploid deletion collection (LIfe Technologies Inc., now ThermoFisher Scientific, Inc.) and confirmed as both haploid (*MAT**a***) and deleted for the *HSL1* gene using multiple diagnostic PCRs both upstream and downstream of the locus and specific primers to the *Kan^R* cassette. Subsequent strains deleted for *HSL1* were created using chromosomal DNA from this strain as a template to amplify a *hsl1Δ::Kan^R* fragment with flanking UTR sequence.

[d]This strain was generated by swapping the *Kan^R* marker from strain GFY-121 to *Nat^R*.

[e]This strain was created by swapping the *Kan^R* marker from strain GFY-104 to *SpHIS5*.

[f]This strain is derived from GFY-58 and was generated in the presence of a WT *CDC11*-expressing *URA3*-marked plasmid, pJT1520. Two rounds of selection on media containing 5-FOA was used to remove the covering vector.

[g]The mCherry tag is placed in-frame after the K391N mutation within the *cdc12-6* allele (Finnigan et al., 2015a).

[h]These strains were constructed by integrating the tagged *HSL1* allele at the endogenous *HSL1* locus in strain GFY-1156 using overlapping PCR fragments of the entire *HSL1* cassette (first generated on plasmids pGF-IVL787 through pGF-IVL792) including the C-terminal epitope tag and drug resistance marker.

[i]For clarity, the residues present within the resulting Hsl1 protein are presented for each construct, rather than the residues deleted.

Table S2. Plasmids used to obtain the data in Figures S1 to S7.

Plasmid	Description	Reference
pGF-IVL521[a,b]	pRS315 *prCDC11::HSL1(1-1518)::eGFP::Kan^R*	This study
pGF-IVL524	pRS315 *prCDC11::hsl1(1358-1518)::eGFP::Kan^R*	This study
pGF-IVL667	pRS315 *prCDC11::hsl1(1-1143; 1201-1518)::eGFP::Kan^R*	This study
pGF-IVL775	pRS315 *prCDC11::hsl1(1-950; 1044-1518)::eGFP::Kan^R*	This study
pGF-IVL776	pRS315 *prCDC11::hsl1(1-950; 1201-1518)::eGFP::Kan^R*	This study
pGF-IVL777	pRS315 *prCDC11::hsl1(1-950; 1358-1518)::eGFP::Kan^R*	This study
pGF-IVL778	pRS315 *prCDC11::hsl1(1-1044; 1358-1518)::eGFP::Kan^R*	This study
pGF-IVL536	pRS315 *prCDC11::hsl1(611-950; 1245-1518)::eGFP::Kan^R*	This study
pGF-IVL652[c]	pRS315 *prCDC11::hsl1(611-950 K775A E776A N777A)::eGFP::Kan^R*	This study
pGF-IVL653[d]	pRS315 *prCDC11::hsl1(611-950 R828A L831A)::eGFP::Kan^R*	This study
pGF-IVL654	pRS315 *prCDC11::hsl1(611-950 K775A E776A N777A R828A L831A)::eGFP::Kan^R*	This study
pGF-IVL655	pRS315 *prCDC11::hsl1(611-950; 1245-1518 K775A E776A N777A)::eGFP::Kan^R*	This study
pGF-IVL656	pRS315 *prCDC11::hsl1(611-950; 1245-1518 R828A L831A)::eGFP::Kan^R*	This study
pGF-IVL657	pRS315 *prCDC11::hsl1(611-950; 1245-1518 K775A E776A N777A R828A L831A)::eGFP::Kan^R*	This study
pGF-IVL612	pRS315 *prCDC11::hsl1(611-950)::eGFP::Kan^R*	This study
pGF-IVL672[e]	pRS315 *prCDC11::hsl1(611-710)::GST::MBP::eGFP::Kan^R*	This study
pGF-IVL774[f]	pRS316 *prCDC11::HSL1(1-1518)::eGFP::Nat^R*	This study
pGF-preIVL51	pRS315 *prCDC11::CDC11::eGFP::Hyg^R*	This study
pGF-IVL650[g]	pRS315 *prCDC11::eGFP::HSL7::SpHIS5*	This study
pGF-IVL672[h]	pRS315 *prCDC11::hsl1(611-710)::GST::MBP::eGFP::Kan^R*	This study
pGF-IVL673	pRS315 *prCDC11::GST::MBP::eGFP::SpHIS5*	This study
pGF-IVL701	pRS315 *prCDC11::hsl1(611-710 R635A R636A K645A H648A K649A R653A K654A)::GST::MBP::eGFP::Kan^R*	This study

pGF-IVL750	pRS315 *prCDC11::hsl1(611-710 R635A R636A K645A H648A K649A R653A K654A R663A R664A K672A R673A K683A R684A)::GST::MBP::eGFP::Kan^R*	This study
pGF-IVL756	pRS315 *prCDC11::hsl1(711-950)::GST::MBP::eGFP::Kan^R*	This study
pGF-IVL753	pRS315 *prCDC11::hsl1(744-950)::GST::MBP::eGFP::Kan^R*	This study
pGF-IVL754	pRS315 *prCDC11::hsl1(800-950)::GST::MBP::eGFP::Kan^R*	This study
pGF-IVL755	pRS315 *prCDC11::hsl1(850-950)::GST::MBP::eGFP::Kan^R*	This study
pGF-IVL821	pRS315 *prCDC11::hsl1(611-710 T665A L666A N668A S669A S671A K672A R673A S674A L675A Y676A S677A S680A I681A S682A K683A R684A S685A N687A L688A)::GST::MBP::eGFP::Kan^R*	This study

[a]For clarity, rather than present the deleted residues, the numbering system for alleles of *HSL1* present the amino acid resides still present within the final protein sequence.

[b]For variants of Hsl1 that include the *CDC11* promoter and are C-terminally tagged with *eGFP::Kan^R*, the following construction strategy was utilized to aid in plasmid generation. First, a parent vector (pGF-IVL520) was generated that contained *prCDC11::eGFP::Kan^R* with a unique *NotI* restriction site between the promoter sequence and the first codon of eGFP. *In vivo* ligation and homologous transformation was used to gap repair the linearized parent vector to insert the fragment(s) of *HSL1* sequence. Additionally, due to the large size of the *HSL1* gene, multiple PCRs were often generated containing a significant amount (several hundred bases) of homology to link adjacent fragments.

[c]The identified KEN box motif K-E-N-X_3-E/D/N (Burton and Solomon, 2001) had residues K775 E776 and N777 mutated to Ala.

[d]The identified destruction (D) box motif R-X_2-L-X_4-N/D/E (Burton and Solomon, 2001) had residues R828 and L831 mutated to Ala.

[e]The GST and MBP tags were amplified from vectors pJT4649 and pJT3239, respectively. Additionally, the MBP tag has the amino acid sequence "NSSSARL" appended to its C-terminus.

[f]This plasmid was built using *in vivo* ligation and homologous recombination; *pRS316::prCDC11* (pGF-V106) was used as the parental vector. The Hsl1 sequence also contains a point mutation (W923R) found within a poorly conserved region (Figure S2) that does not alter its bud neck localization.

[g]The parental vector for this plasmid was *pRS315::prCDC11* (pGF-V201).

[h]The GST and MBP tags were amplified from vectors pJT4649 and pJT3239, respectively. Additionally, the MBP tag has the amino acid sequence “NSSSARL” appended to its C-terminus.

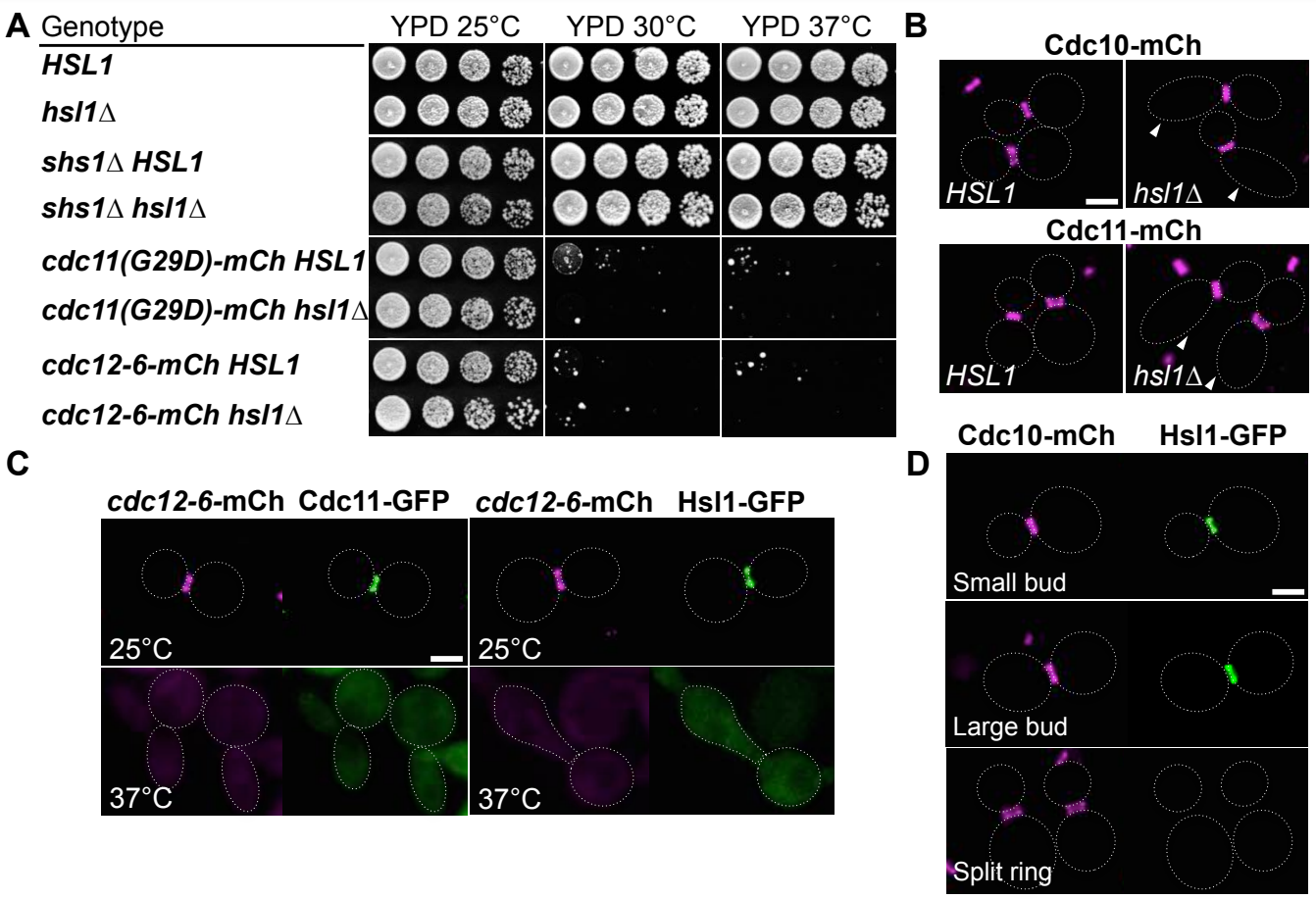

FIGURE S1. Checkpoint kinase Hsl1 is recruited to the bud neck in a septin-dependent manner. (A) Overnight cultures (grown at 25°C) of the indicated genotypes (yeast strains BY4741, GFY-1541, GFY-39, GFY-1451, GFY-1120, GFY-1450, GFY-1430 and GFY-1449) were spotted in five-fold serial dilution onto rich medium plates and grown at the indicated temperatures for 2 days (37°C) or 3 days (25°C, 30°C), then imaged. All strains were selected twice on synthetic complete medium containing 5-FOA to counter-select for the WT covering plasmids [at room temperature, for strains harboring the *cdc11(G29D)* or *cdc12-6* alleles] prior to being cultured for the growth assays. Absence of Shs1 has non-lethal, but readily detectable, effects on septin collar structure and function (Garcia et al., 2011; Finnigan et al., 2015b). The *cdc11(G29D)* allele is compromised for its G interface-mediated association with Cdc12 and is inviable at elevated temperature (Weems et al., 2014; Finnigan et al., 2015b). The *cdc12-6* allele causes rapid dissolution of the entire septin collar and is also inviable at elevated temperature (Finnigan et al., 2015a; Johnson et al., 2015). (B) Exponentially-growing cultures (30°C) of the indicated genotype which express a mCherry-tagged copy of Cdc10 (GFY-42 and GFY-1156) or Cdc11 (GFY-768 and GFY-1157) from the corresponding endogenous locus were visualized by fluorescent microscopy. Yeast were grown on 5-FOA twice as in (A) prior to culturing. Dotted white lines, cell periphery. *Scale bar*, 2 μM. Arrowheads, cells with elongated morphology. (C) Yeast expressing an mCh-tagged derivative of the *cdc12-6*^{ts} allele (GFY-104) were transformed with vectors expressing either Cdc11-GFP (pGF-preIVL51, *left*) or Hsl1-GFP (pGF-IVL521, *right*) and selected on SD-LEU+5-FOA medium twice to remove the WT *CDC12*-expressing vector. Cultures were grown to exponential phase at 25°C and shifted to the restrictive temperature (37°C) for 1 h prior to collecting cells and imaging by fluorescent microscopy. Representative images are presented and all were scaled identically as in (B). *Scale bar*, 2 μM. (D) Cells from different stages of the cell division cycle in a strain expressing both Cdc10-mCherry (GFY-42) and Hsl1-GFP (from vector pGF-IVL521) were imaged as in (B). Scale bar, 2 μM.

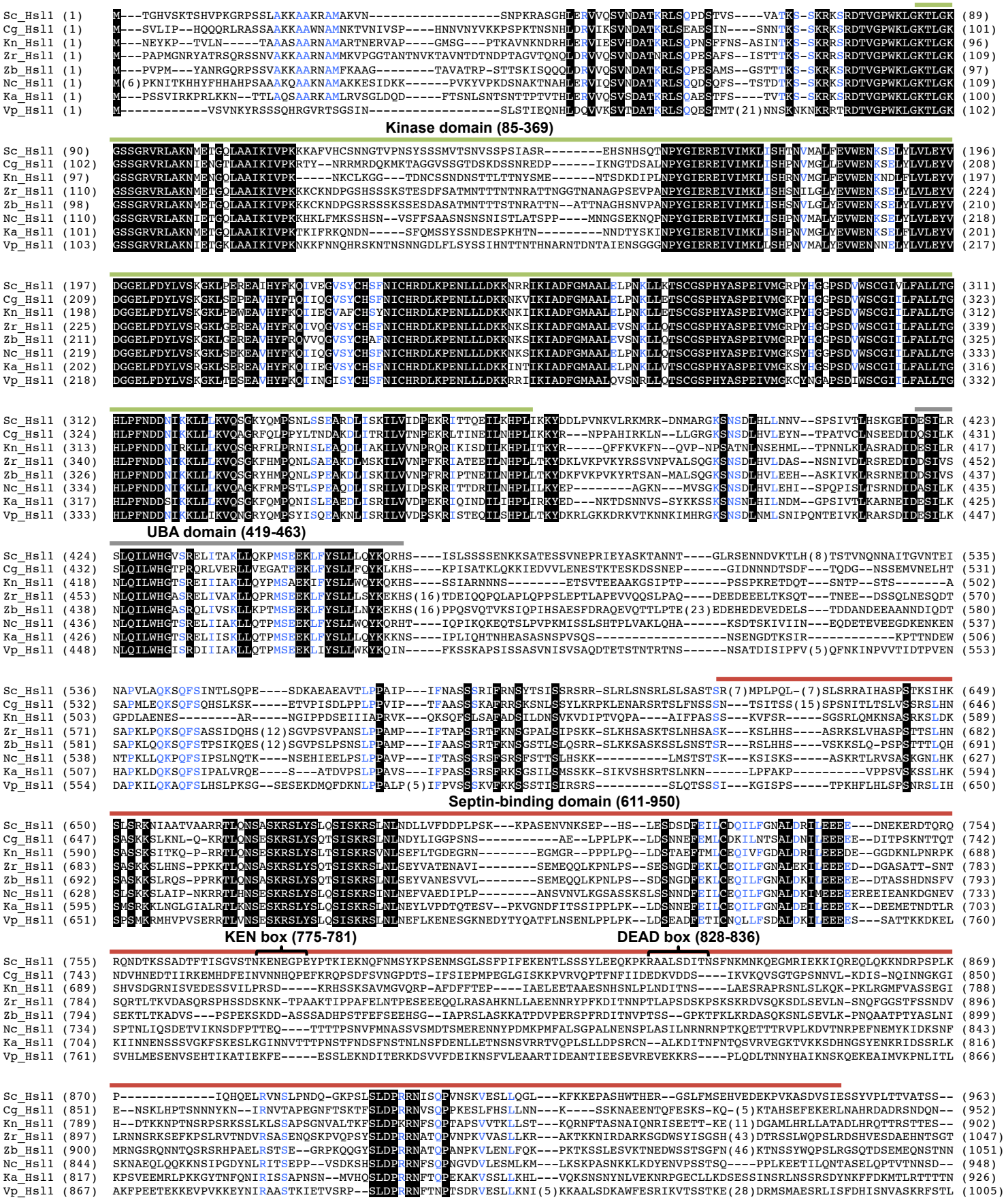
Kinase domain (85-369)
UBA domain (419-463)
Septin-binding domain (611-950)
KEN box (775-781)
DEAD box (828-836)

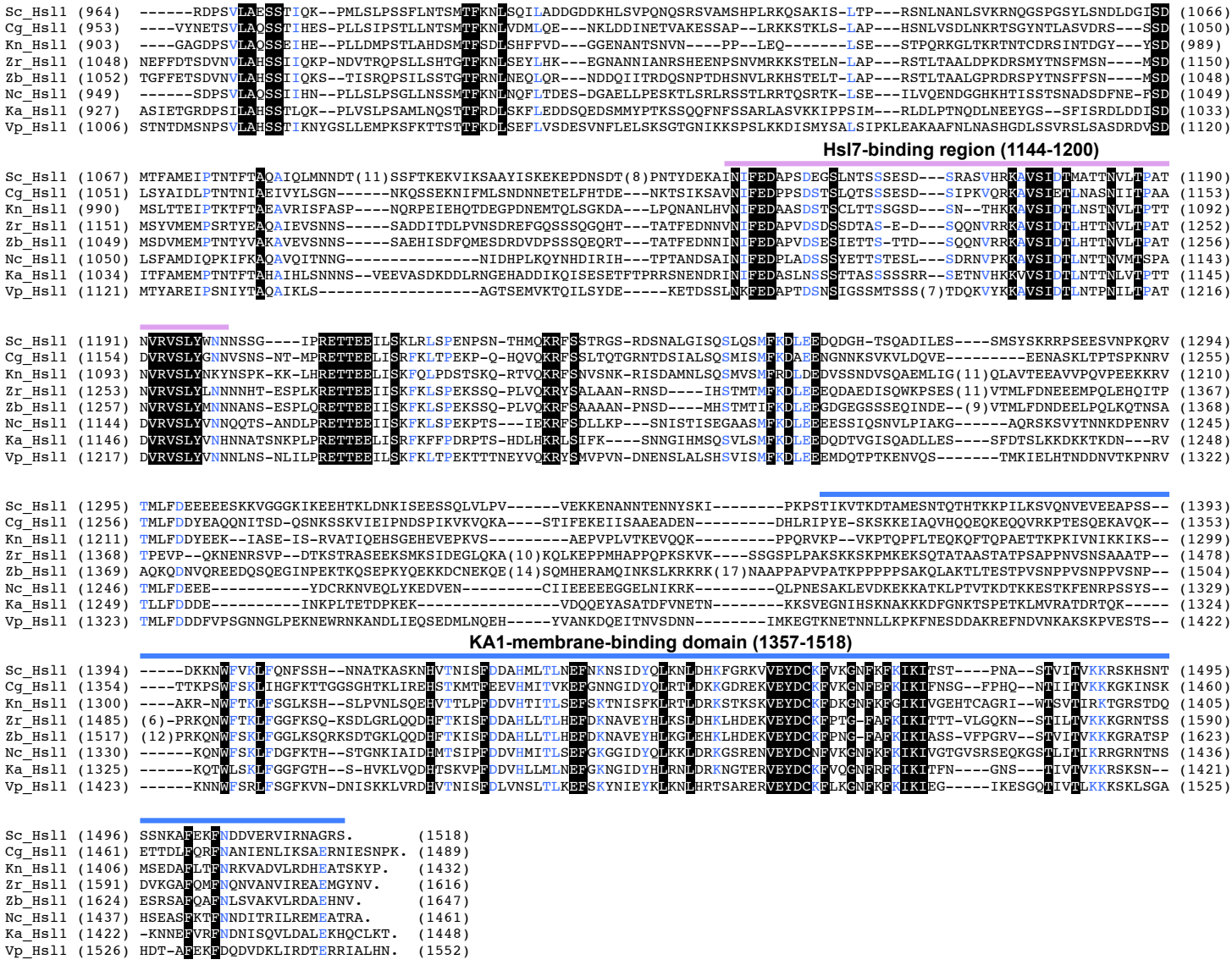

FIGURE S2. Alignment of Hsl1 orthologs from various yeast species. CLUSTAL-W (Thompson et al., 1994) was used to align Hsl1 proteins (residue numbers in parentheses) from: Sc, *Saccharomyces cerevisiae*; Cg, *Candida glabrata*; Kn, *Kazachstania naganishii*; Zr, *Zygosaccharomyces rouxii*; Zb, *Zygosaccharomyces bailii*; Nc, *Naumovozyma castellii*; Ka, *Kazachstania africana*; and Vp, *Vanderwaltozyma polyspora*. Location of various domains and sequence elements are indicated: Kinase domain (85-369) (Russell and Nurse, 1987); UBA domain (410-462) (Hofmann and Bucher, 1996; Mueller and Feigon, 2002); septin-binding domain (611-950) (this study); KEN box (775-781) and D-box (849-857) (Burton and Solomon, 2001); Hsl7-binding sequence (1144-1200) (Shulewitz et al., 1999; Shulewitz, 2000; Crutchley et al., 2009), and the KA1 domain (1357-1518) (Moravcevic et al., 2010). White-on-black letters, residues invariant across all eight fungal species; blue letters, residues strongly conserved (found in 7 of the 8 species).

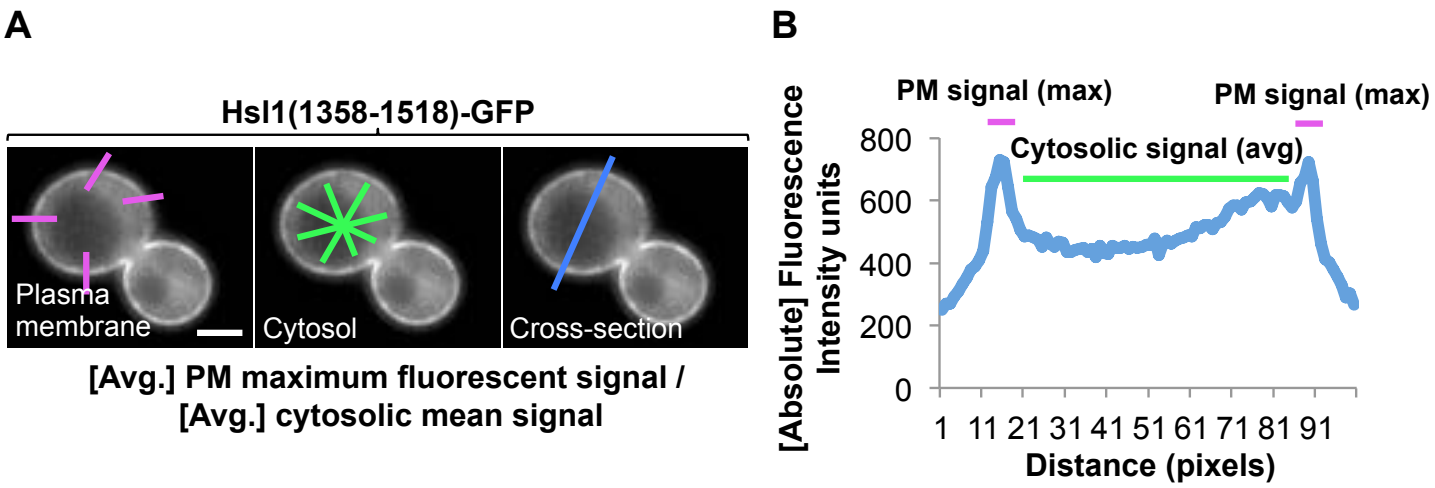

FIGURE S3. Quantification of GFP fluorescence at the plasma membrane using ImageJ. (A) A strain expressing Cdc10-mCherry (GFY-42), and harboring a plasmid expressing the KA1 domain of Hsl1(1357-1518) fused to GFP (pGF-IVL524) as a plasma membrane (PM) marker, is used here as an example. First, for each cell, four randomly placed lines were drawn across the cell periphery (*left panel*, pink lines). The maximal / peak pixel intensity of each line represents the PM contribution. Second, four lines were randomly drawn within the cell body excluding the PM (*middle panel*, green lines). To calculate the PM-to-cytosolic ratio, the average maximum PM pixel intensity was divided by the mean cytosolic intensity. *Scale bar*, 2 μM. (B) The pixel intensity profile of a single line scan across the same cell used in (A) indicating the portions corresponding to the PM peaks (pink) and the cytosolic region (green) described in (A). In the calculation of the PM-to-cytosolic ratio, no subtraction of background fluorescence (black) was included.

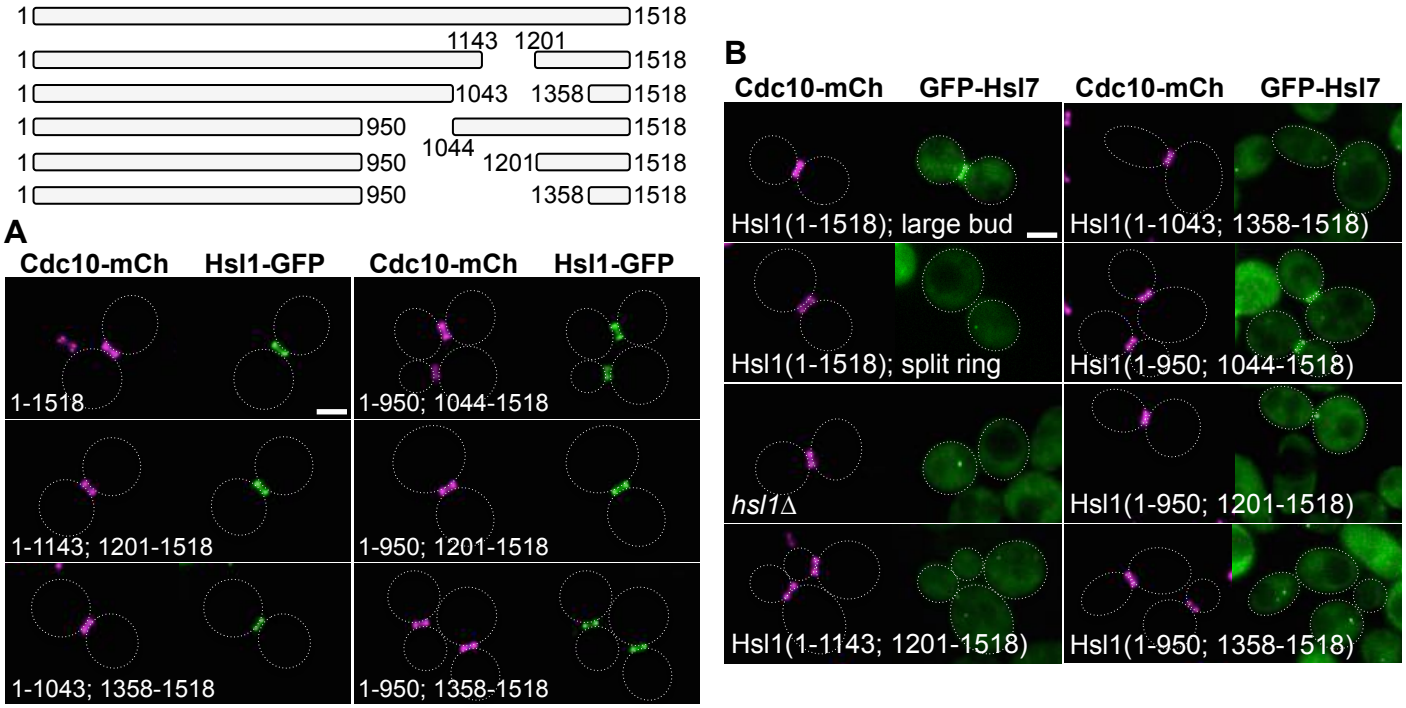

FIGURE S4. Bud neck recruitment of Hsl7 requires its interaction with a short segment of Hsl1 (residues 1144-1200) located between the septin-binding elements and the C-terminal membrane-binding KA1 domain. (A) Plasmids expressing GFP-tagged derivatives of full-length Hsl1 and the indicated set of internal deletions (pGF-IVL521, pGF-IVL667, and pGF-IVL775 through pGF-IVL778) were introduced into a strain (GFY-42) expressing Cdc10-mCherry from the endogenous *CDC10* locus and examined by fluorescence microscopy (all images were scaled identically). Dotted white lines, cell periphery. None of these deletions prevents Hsl1 localization to the septin collar. *Scale bar*, 2 μM. (B) Cells lacking Hsl1 (*hsl1*Δ) or producing the same set of Hsl1 constructs as in (A), expressed from the endogenous *HSL1* locus (and C-terminally tagged with the 3XHA epitope, instead of GFP, to permit confirmation of expression) in cells also expressing Cdc10-mCherry from the endogenous *CDC10* locus (strains GFY-1561 through GFY-1566) were transformed with a vector expressing N-terminally tagged GFP-Hsl7 (pGF-IVL650) and imaged by fluorescence microscopy as in (A). *Scale bar*, 2 μM. The Hsl1 constructs that lack any portion of the region 1144-1200 fail to recruit Hsl7 to the bud neck prior to splitting of the septin collar and, instead, GFP-Hsl7 localizes as a single dot. It has been demonstrated before that this single dot is the spindle pole body; when Hsl1 is absent (after its APC-mediated destruction upon the onset of anaphase and until early G1, or in an *hsl1*Δ mutant or, as shown here, in Hsl1 mutants that cannot bind Hsl7), Hsl7 localizes to the spindle pole body and not the bud neck (Shulewitz et al., 1999; Shulewitz, 2000; Cid et al., 2001).

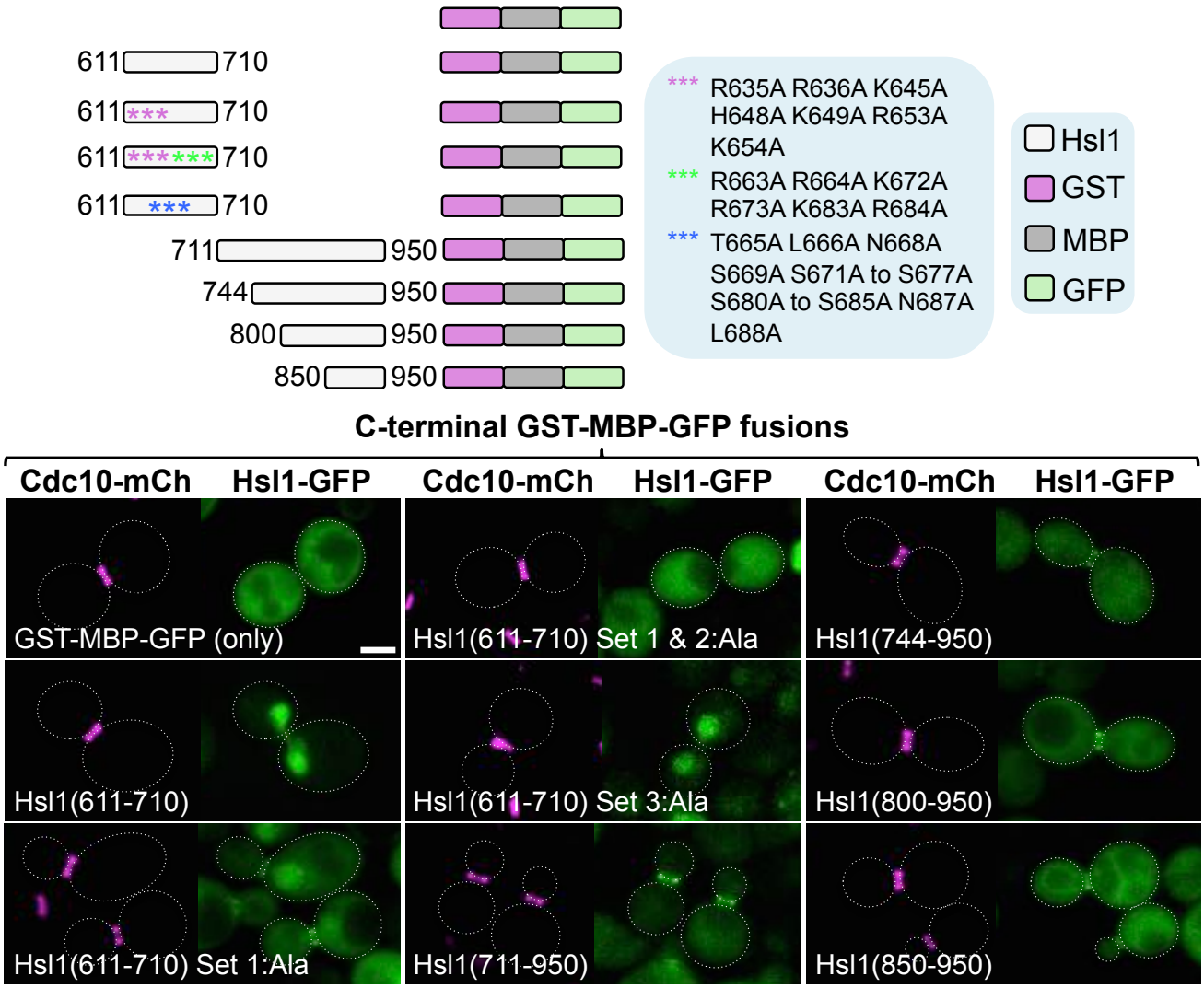

FIGURE S5. A triple protein fusion localization assay demonstrates that residues 611-950 in Hsl1 contain a cryptic NLS and at least two separable elements sufficient to support bud neck recruitment. A plasmid (pGF-IVL672) expressing a GST-MBP-eGFP chimera and derivatives in which the indicated fragments of Hsl1 were fused to its N-terminus (pGF-IVL673, pGF-IVL701, pGF-IVL750, pGF-IVL753 through pGF-IVL756, and pGF-IVL821) were introduced into a strain expressing Cdc10-mCherry (GFY-42) and visualized by fluorescent microscopy (all images were scaled identically). Dotted white lines, cell periphery. *Scale bar*, 2 μM. The GST-MBP-eGFP chimera is excluded from the nucleus (*left column*, upper panel), whereas an Hsl1(611-710)-GST-MBP-eGFP fusion exhibits efficient nuclear import (*left column*, middle panel). Mutation to Ala of the seven basic residues (Set 1) in an apparent classical bipartite NLS (635**RR**AIHASPST**K**SI-**HK**SLS**RK**654) (Robbins et al., 1991) in the same fusion largely abrogates nuclear entry and reveals retention at the bud neck (*left column*, lower panel). Mutation to Ala of additional basic residues within a conserved region downstream (Set 1 & Set 2) prevents both nuclear import and bud neck localization (*middle column*, upper panel), suggesting that the conserved region (residues 663-688, see Fig. S2) contains residues important for septin binding. In agreement, mutation to Ala of only those conserved residues (Set 3) allows nuclear import (*middle column*, lower panel). An Hsl1(711-950)-GST-MBP-eGFP fusion shows robust retention at the bud neck (*middle column*, bottom panel), even when progressively pared down to ~100 residues (850-950) (*middle column*, top, middle and lower panel), which also contain a small conserved element (residues 877-910, see Fig. S2).

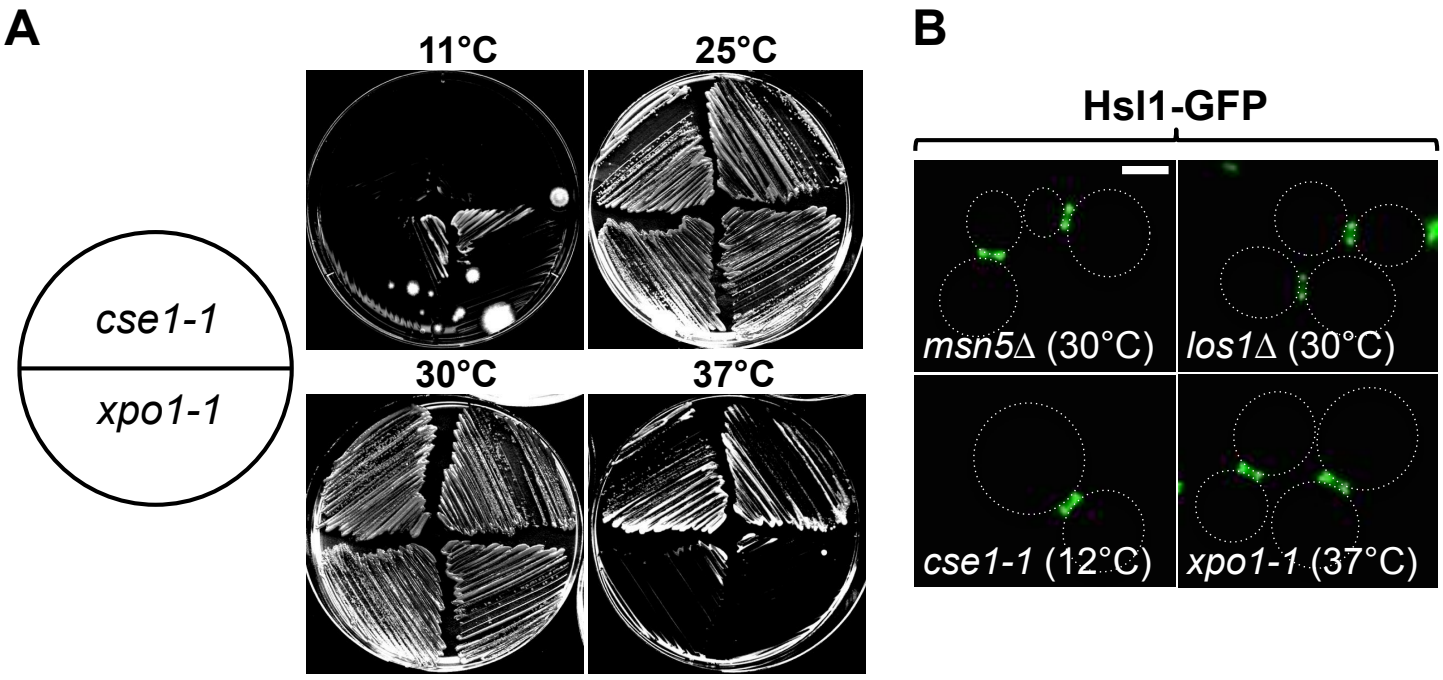

FIGURE S6. Native Hsl1 likely does not normally undergo nucleocytoplasmic shuttling. We tested whether Hsl1 would accumulate in the nucleus in any strain lacking the function of one of the four known karyopherins that mediate nuclear export ("exportins") of various classes of proteins (Strom and Weis, 2001; Strahl et al., 2005). Although *los1*Δ and *msn5*Δ strains are viable, *CSE1* and *XPO1/CRM1* are essential genes; hence, we acquired, tested and confirmed the phenotypes of strains carrying either a cold-sensitive allele (*cse1-1*) of the former (Panel A, *upper half*) or a temperature-sensitive allele (*xpo1-1*) of the latter (Panel A, *lower half*). Two colonies of each of the indicated strains were streaked on rich medium (YPD) plates and incubated for either 4 days (25°, 30°, and 37°C) or 14 days (11°C). (B) Both the *cse1-1* and *xpo1-1* strains contained an *ade2* mutation, which causes intracellular accumulation of a red pigment that increases the intrinsic background fluorescence of the cells and also moderately impairs growth even on plates containing adenine (Weisman et al., 1987). To eliminate the background fluorescence problem, the *cse1-1* and *xpo1-1* strains were streaked for single colonies and spontaneous white derivatives that do not accumulate the red pigment (because they have acquired a mutation in a gene for an enzyme that acts further upstream in the adenine pathway) (Ugolini and Bruschi, 1996) were picked for subsequent use. Each of the exportin-defective strains was transformed with a *URA3*-marked plasmid (pGF-IVL774) expressing Hsl1-GFP and selected on SD-Ura (+Ade, where necessary) plates at 30°C. Exponentially-growing cultures of the *los1*Δ and *msn5*Δ cells expressing Hsl1-GFP were visualized by fluorescence microscopy at 30°C. Strains harboring the *cse1-1* or *xpo1-1* mutations were cultured overnight at 25°C, back diluted to an $A_{600\ nm}$ = ~0.3 for 5 h, and then shifted to the restrictive temperature (either 12°C or 37°C, respectively) for 6 h and then imaged. Dotted white lines, cell periphery. *Scale bar*, 2 μM. No nuclear accumulation was observed in any of the exportin-deficient cells. Thus, unlike other cell cycle regulators (Keaton et al., 2008), Hsl1 does not appear to undergo nucleocytoplasmic shuttling.

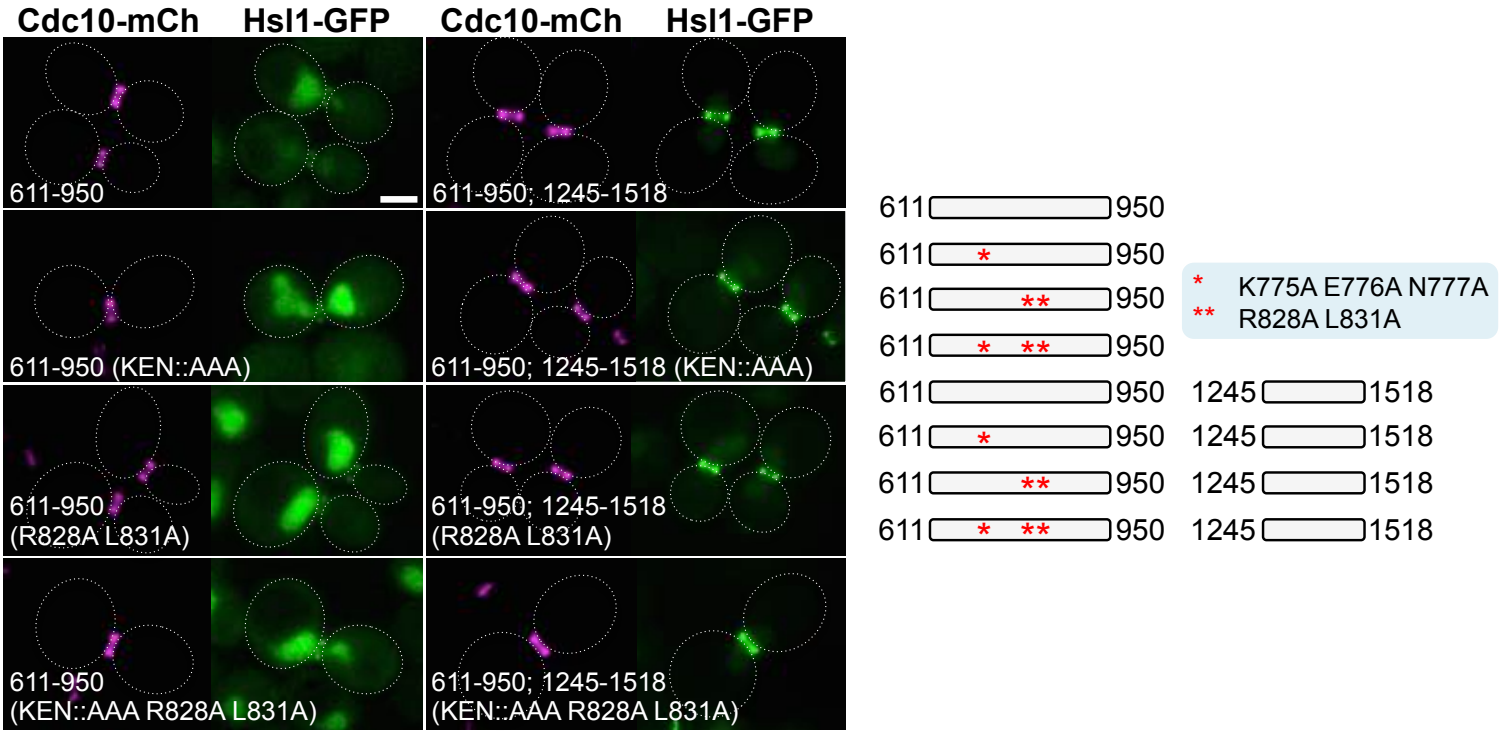

FIGURE S7. The KEN box and D box are not required for localization of the bud neck-associated fragment Hsl1(611-950). The KEN box motif (K-E-N-X_3-E/D/N; residues 775-781) and the D box motif (R-X_2-L-X_4-N/D/E; residues 828-836) required for APC-mediated ubiquitinylation and subsequent degradation of Hsl1 were characterized previously (Burton and Solomon, 2001). Native Hsl1(611-950) alone (*left column*) or fused at its C-terminus to a C-terminal fragment containing the Hsl1 KA1 domain (*right column*), or derivatives containing the indicated mutational alterations of the key residues in the KEN box and/or D-box motifs (pGF-IVL536, pGF-IVL612, and pGF-IVL652 through pGF-IVL657) were expressed in a strain (GFY-42) co-expressing Cdc10-mCherry and imaged by fluorescence microscopy (all images were scaled identically), Dotted white lines, cell periphery. *Scale bar*, 2 μM. Regardless of any alteration of the KEN and/or D box, Hsl1(611-950) localizes weakly to the bud neck, but predominantly to the nucleus due to the action of its cryptic NLS (see Fig. S5). Likewise, regardless of any alteration of the KEN and/or D box, Hsl1(611-950; 1245-1518) localizes exclusively to the bud neck (because presence of the KA1 domain prevents nuclear entry, presumably by first retaining the protein at the PM prior to its association with the septin collar. Results shown in Fig. 2D eliminate the possibility that presence of a cryptic potential NES, L-X-I-X_3-L-X_2-M (residues 1245-1254), contributes to the behavior of Hsl1(611-950; 1245-1518).

SUPPLEMENTAL REFERENCES

Brachmann, C.B., Davies, A., Cost, G.J., Caputo, E., Li, J., Hieter, P., and Boeke, J.D. (1998). Designer deletion strains derived from *Saccharomyces cerevisiae* S288C: a useful set of strains and plasmids for PCR-mediated gene disruption and other applications. Yeast *14*, 115-132.

Burton, J.L., and Solomon, M.J. (2001). D box and KEN box motifs in budding yeast Hsl1p are required for APC-mediated degradation and direct binding to Cdc20p and Cdh1p. Genes Dev *15*, 2381-2395.

Crutchley, J., King, K.M., Keaton, M.A., Szkotnicki, L., Orlando, D.A., Zyla, T.R., Bardes, E.S., and Lew, D.J. (2009). Molecular dissection of the checkpoint kinase Hsl1p. Mol Biol Cell *20*, 1926-1936.

Finnigan, G.C., Booth, E.A., Duvalyan, A., Liao, E.N., and Thorner, J. (2015a). The Carboxy-Terminal Tails of Septins Cdc11 and Shs1 Recruit Myosin-II Binding Factor Bni5 to the Bud Neck in *Saccharomyces cerevisiae*. Genetics *200*, 843-862.

Finnigan, G.C., Takagi, J., Cho, C., and Thorner, J. (2015b). Comprehensive Genetic Analysis of Paralogous Terminal Septin Subunits Shs1 and Cdc11 in *Saccharomyces cerevisiae*. Genetics *200*, 821-841.

Garcia, G., 3rd, Bertin, A., Li, Z., Song, Y., McMurray, M.A., Thorner, J., and Nogales, E. (2011). Subunit-dependent modulation of septin assembly: budding yeast septin Shs1 promotes ring and gauze formation. J Cell Biol *195*, 993-1004.

Hofmann, K., and Bucher, P. (1996). The UBA domain: a sequence motif present in multiple enzyme classes of the ubiquitination pathway. Trends Biochem Sci *21*, 172-173.

Johnson, C.R., Weems, A.D., Brewer, J.M., Thorner, J., and McMurray, M.A. (2015). Cytosolic chaperones mediate quality control of higher-order septin assembly in budding yeast. Mol Biol Cell *26*, 1323-1344.

Keaton, M.A., Szkotnicki, L., Marquitz, A.R., Harrison, J., Zyla, T.R., and Lew, D.J. (2008). Nucleocytoplasmic trafficking of G2/M regulators in yeast. Mol Biol Cell *19*, 4006-4018.

Moravcevic, K., Mendrola, J.M., Schmitz, K.R., Wang, Y.H., Slochower, D., Janmey, P.A., and Lemmon, M.A. (2010). Kinase associated-1 domains drive MARK/PAR1 kinases to membrane targets by binding acidic phospholipids. Cell *143*, 966-977.

Mueller, T.D., and Feigon, J. (2002). Solution structures of UBA domains reveal a conserved hydrophobic surface for protein-protein interactions. J Mol Biol *319*, 1243-1255.

Robbins, J., Dilworth, S.M., Laskey, R.A., and Dingwall, C. (1991). Two interdependent basic

domains in nucleoplasmin nuclear targeting sequence: identification of a class of bipartite nuclear targeting sequence. Cell *64*, 615-623.

Russell, P., and Nurse, P. (1987). The mitotic inducer nim1+ functions in a regulatory network of protein kinase homologs controlling the initiation of mitosis. Cell *49*, 569-576.

Shulewitz, M.J. (2000). Septin assembly regulates cell cycle progression through activation of a protein kinase signaling pathway. Ph.D. Dissertation, Dept of Molecular and Cell Biology, Univ. of California, Berkeley, 172pp.

Shulewitz, M.J., Inouye, C.J., and Thorner, J. (1999). Hsl7 localizes to a septin ring and serves as an adapter in a regulatory pathway that relieves tyrosine phosphorylation of Cdc28 protein kinase in *Saccharomyces cerevisiae*. Mol Cell Biol *19*, 7123-7137.

Strahl, T., Hama, H., DeWald, D.B., and Thorner, J. (2005). Yeast phosphatidylinositol 4-kinase, Pik1, has essential roles at the Golgi and in the nucleus. The J Cell Biol *171*, 967-979.

Strom, A.C., and Weis, K. (2001). Importin-beta-like nuclear transport receptors. Genome Biol *2*, Reviews3008.

Thompson, J.D., Higgins, D.G., and Gibson, T.J. (1994). CLUSTAL W: improving the sensitivity of progressive multiple sequence alignment through sequence weighting, position-specific gap penalties and weight matrix choice. Nucleic Acids Res *22*, 4673-4680.

Ugolini, S., and Bruschi, C.V. (1996). The red/white colony color assay in the yeast *Saccharomyces cerevisiae*: epistatic growth advantage of white *ade8-18*, *ade2* cells over red *ade2* cells. Curr Genet *30*, 485-492.

Weems, A.D., Johnson, C.R., Argueso, J.L., and McMurray, M.A. (2014). Higher-order septin assembly is driven by GTP-promoted conformational changes: evidence from unbiased mutational analysis in *Saccharomyces cerevisiae*. Genetics *196*, 711-727.

Weisman, L.S., Bacallao, R., and Wickner, W. (1987). Multiple methods of visualizing the yeast vacuole permit evaluation of its morphology and inheritance during the cell cycle. The J of Cell Biol *105*, 1539-1547.